Shifts in the temperature of maximum density (TMD) of ionic liquid aqueous solutions

5 AUTHORS, INCLUDING:

Tariq Mohammad
Qatar University
51 PUBLICATIONS **567** CITATIONS

SEE PROFILE

José Esperança
New University of Lisbon
110 PUBLICATIONS **4,490** CITATIONS

SEE PROFILE

Jose Nuno A Canongia Lopes
Technical University of Lisbon
179 PUBLICATIONS **8,341** CITATIONS

SEE PROFILE

PAPER

Shifts in the temperature of maximum density (TMD) of ionic liquid aqueous solutions†

M. Tariq,*[a] J. M. S. S. Esperança,[a] M. R. C. Soromenho,[a] L. P. N. Rebelo[a] and J. N. Canongia Lopes*[ab]

This work investigates for the first time shifts in the temperature of maximum density (TMD) of water caused by ionic liquid solutes. A vast amount of high-precision volumetric data—more than 6000 equilibrated (static) high-precision density determination corresponding to ~90 distinct ionic liquid aqueous solutions of 28 different types of ionic liquid—allowed us to analyze the TMD shifts for different homologous series or similar sets of ionic solutes and explain the overall effects in terms of hydrophobic, electrostatic and hydrogen-bonding contributions. The differences between the observed TMD shifts in the $-2 < t/°C < 4$ range and salting-in or salting-out effects produced by the same type of ions in aqueous solutions at higher temperatures are discussed taking into account the different types of possible solute–water interactions that can modify the structure of the aqueous phase. The results also reveal different insights concerning the nature of the ions that constitute typical ionic liquids and are consistent with previous results that established hydrophobic and hydrophilic scales for ionic liquid ions based on their specific interactions with water and other probe molecules.

Introduction

Water is a simple, symmetric molecule. Yet liquid water is a complex, wondrous fluid, essential for life on Earth, as we know it. The unique properties of water derive from an intricate balancing act that tries to accommodate its ability to perform multiple hydrogen-bond (HB) interactions within a rather limited amount of space. One of the most well known consequences of such subtle balance is the open structure of ice (think of delicate ice crystals) and the concomitant density increase upon melting (+9%). Even in the liquid state the intricate hydrogen-bonded structure is not entirely lost; pure water continues to contract until a temperature of maximum density (TMD) is reached around 4 °C (the density increases +0.013% between 0 and 4 °C).[1]

Shifts in the TMD of water solutions ($\Delta\theta$) are an effective way to probe the nature of the hydrogen-bonded structure of those solutions; solutes that promote a more stable HB network should yield solutions with higher TMDs, whereas those that break the HB network should decrease the TMD value.

In most cases, the $\Delta\theta$ values are proportional to the amount of added solute, as stated by the Despretz rule.[2,3] It must be stressed that such a rule does not entail a colligative property such as the freezing point depression of aqueous solutions; whereas the latter property does not depend on the nature of the solute (just on its added amount), the shifts in the TMD of the aqueous solutions will depend on the ability of different solutes to interfere with the HB network of liquid water. Moreover, the Despretz rule should be understood as a limiting law; in the absence of solute–solute interactions (low solute concentrations) the amount of interference with the HB network of water should be proportional to the amount and nature of the solute present; that is not necessarily the case for more concentrated solutions or for solutes that tend to self-aggregate even at fairly low concentrations (e.g. surfactant molecules with long alkyl chains). Finally, most authors[4–10] have dissected the observed TMD shifts into two contributions: $\Delta\theta = \Delta\theta_{id} + \Delta\theta_{st}$. The ideal shift, $\Delta\theta_{id}$, is proportional to the concentration, molar volume and thermal expansion of the pure solute, and incorporates the part of the shift that is simply caused by the addition to water of a solute that (as most pure substances) tends to expand as temperature increases. Such shift is always negative and (for similar thermal expansion coefficients) is directly proportional to the molar volume of the solute. The correct dissection of $\Delta\theta$, via the calculation of the $\Delta\theta_{id}$ term, allows the comparison between different solutes, separating

[a] Instituto de Tecnologia Química e Biológica, Universidade Nova de Lisboa, Av. da República, 2780-157 Oeiras, Portugal. E-mail: tariq@itqb.unl.pt, jnlopes@ist.utl.pt; Web: www.itqb.unl.pt
[b] Centro de Química Estrutural, Instituto Superior Tecnico, 1049-001 Lisboa, Portugal
† Electronic supplementary information (ESI) available. See DOI: 10.1039/c3cp50387a

the effects caused by their different sizes and expansion rates from those that correspond to different solute–water interactions (the $\Delta\theta_{st}$ structural term).

Many inorganic and organic compounds have been used as solutes within the framework of TMD shifts.[1,9] Most studied solutions produce negative $\Delta\theta$ values and it is usually possible to correlate the observed trends with the size or charge density within a given homologous series of solutes; for instance halogen salts with a common cation generally follow the order $\Delta\theta(I^-) > \Delta\theta(Br^-) > \Delta\theta(Cl^-)$.[4] A most curious exception to this state of affairs comes from ethanol and propanol solutions that exhibit non-linear, non-monotonous trends of $\Delta\theta$ as a function of solute concentration (positive $\Delta\theta$ values at low concentrations, negative at higher concentrations). In fact it was shown[5] that after taking into account the $\Delta\theta_{id}$ term, the remainder $\Delta\theta_{st}$ structural term reflects the amount of specific water–solute interactions that are possible to maintain in systems where the solutes can promote multiple hydrogen bonding and even the formation of clathrate hydrates.

Those studies, ranging from ionic to molecular solutes, have shown that when a solute is added to water the resulting TMD shifts can be discussed not only in terms of the HB network of water but also (and more importantly) how the different possible solute–water interactions—coulomb interactions, hydrogen bonds, hydrophobic effects—must be balanced in order to yield the observed outcome.

Ionic liquids are a novel class of ionic compounds characterized by melting point temperatures below 100 °C. Unlike most traditional inorganic salts, ionic liquids are generally composed of flexible, alkyl-substituted, asymmetric, and/or charge-dispersed ions that prevent the interactions within the fluid, which are completely dominated by coulomb interactions. In fact, pure ionic liquids can be rationalized as dual, nano-structured fluids composed of a malleable polar network—an array of the charged parts of the ions interacting *via* coulomb interactions—permeated by non-polar domains subject to dispersion forces.[11,12] Some ionic liquid ions also contain groups capable of acting as hydrogen-bond donors or acceptors.

Such versatility in terms of interactions of the ions that compose most ionic liquids coupled with the distinctive properties of the resulting media led us to the issue of their behavior in aqueous solution and to the determination for the first time of the corresponding TMD shifts. The resulting volumetric data—28 different ionic liquids and their aqueous solutions—will be presented and discussed in the following sections.

Experimental

Materials

The 28 ionic liquids used in the present work were either purchased or synthetized at the Queens University Ionic Liquids Laboratory, Belfast, UK[13,14] or at Instituto de Tecnologia Química e Biológica, Oeiras, Portugal.[15,16] Table 1 lists their origin and stated purity, along with the acronyms used throughout the work and the corresponding structural formulas.

General synthesis of [N$_{1\ 1\ n\ 2(OH)}$]Br. The first step in the synthesis of some of the choline-based ionic liquids used in

this work is the preparation of [N$_{1\ 1\ n\ 2(OH)}$]Br salts. The adequate alkyl halide (C$_n$H$_{2n+1}$Br, n = 2, 3) (1.1 mol equiv.) and 2-dimethylaminoethanol (1.0 mol equiv.) were mixed in a round-bottom flask, dissolved in *n*-hexane, under vigorous stirring, reflux and an N$_2$ atmosphere for several hours (monitored by ^{1}H NMR). The formation of the product can be observed by its precipitation from *n*-hexane. After completion of the reaction, the mixture was then filtered and the reaction product was washed extensively with *n*-hexane in order to remove unreacted compounds and then dried under vacuum. The resulting [N$_{1\ 1\ n\ 2(OH)}$]Br salt (yield 99%) was used without further purification.

[N$_{1\ 1\ 2\ 2(OH)}$]Br. ^{1}H-NMR (D$_2$O, 400 MHz): δ/ppm = 1.87 (t, 3H, CH$_3$-CH$_2$-N(CH$_3$)$_2$-CH$_2$-CH$_2$-OH), 3.13 (s, 6H, CH$_3$-CH$_2$-N(CH$_3$)$_2$-CH$_2$-CH$_2$-OH), 3.45–3.51 (m, 4H, CH$_3$-CH$_2$-N(CH$_3$)$_2$-CH$_2$-CH$_2$-OH), 4.04–4.08 (m, 2H, CH$_3$-CH$_2$-N(CH$_3$)$_2$-CH$_2$-CH$_2$-OH).

[N$_{1\ 1\ 3\ 2(OH)}$]Br. ^{1}H-NMR (D$_2$O, 400 MHz): δ/ppm = 0.98 (t, 3H, CH$_3$-CH$_2$-CH$_2$-N(CH$_3$)$_2$-CH$_2$-CH$_2$-OH), 1.76–1.86 (sxt, 2H, CH$_3$-CH$_2$-CH$_2$-N(CH$_3$)$_2$-CH$_2$-CH$_2$-OH), 3.14 (s, 6H, CH$_3$-CH$_2$-CH$_2$-N(CH$_3$)$_2$-CH$_2$-CH$_2$-OH), 3.33 (t, 2H, CH$_3$-CH$_2$-CH$_2$-N(CH$_3$)$_2$-CH$_2$-CH$_2$-OH), 3.49 (t, 2H, CH$_3$-CH$_2$-CH$_2$-N(CH$_3$)$_2$-CH$_2$-CH$_2$-OH), 4.03–4.07 (m, 2H, CH$_3$-CH$_2$-CH$_2$-N(CH$_3$)$_2$-CH$_2$-CH$_2$-OH).
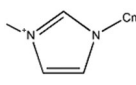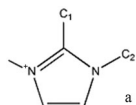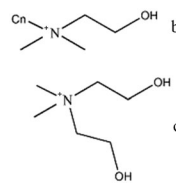
General synthesis of [N$_{1\ 1\ n2(OH)}$][OAc]. An aqueous solution of the [N$_{1\ 1\ 2(OH)}$]Br (n = 2, 3) (1.0 M, 0.025 mol equiv./20 mL resin) salts was eluted in an anionic exchange column of SUPELCO – AMBERLITE$^®$ IRA-78, promoting the formation of the intermediate ionic liquid [N$_{1\ 1\ n2(OH)}$][OH] (n = 2, 3, 4, 5). The anion exchange was followed by the basic pH of the titrating solution, which was used to titrate an equimolar aqueous solution of acetic acid. The titration ceased when the titrating solution presented pH = 7. The solvent was evaporated, and dried under vacuum to obtain the [N$_{1\ 1\ n2(OH)}$][OAc] salts (yield 99%). The absence of halide anions was tested by titration of the ionic liquid sample with a 1.0 M aqueous solution of AgNO$_3$. ^{1}H NMR was used to confirm the purity (99%) of the synthesized ionic liquids.

[N$_{1\ 1\ 2\ 2(OH)}$][OAc]. ^{1}H-NMR (DMSO-d$_6$, 400 MHz): δ/ppm = 1.23 (t, 3H, CH$_3$-CH$_2$-N(CH$_3$)$_2$-CH$_2$-CH$_2$-OH), 1.58 (s, 3H, CH$_3$-(CO)-O), 3.04 (s, 6H, CH$_3$-CH$_2$-N(CH$_3$)$_2$-CH$_2$-CH$_2$-OH), 3.36–3.44 (m, 4H, CH$_3$-CH$_2$-N(CH$_3$)$_2$-CH$_2$-CH$_2$-OH), 3.80–3.84 (m, 2H, CH$_3$-CH$_2$-N(CH$_3$)$_2$-CH$_2$-CH$_2$-OH).

[N$_{1\ 1\ 3\ 2(OH)}$][OAc]. ^{1}H-NMR (D$_2$O, 400 MHz): δ/ppm = 0.88 (t, 3H, CH$_3$-CH$_2$-CH$_2$-N(CH$_3$)$_2$-CH$_2$-CH$_2$-OH), 1.57 (s, 3H, CH$_3$-(CO)-O), 1.65–1.74 (sxt, 2H, CH$_3$-CH$_2$-CH$_2$-N(CH$_3$)$_2$-CH$_2$-CH$_2$-OH), 3.05 (s, 6H, CH$_3$-CH$_2$-CH$_2$-N(CH$_3$)$_2$-CH$_2$-CH$_2$-OH), 3.28 (t, 2H, CH$_3$-CH$_2$-CH$_2$-N(CH$_3$)$_2$-CH$_2$-CH$_2$-OH), 3.37 (t, 2H, CH$_3$-CH$_2$-CH$_2$-N(CH$_3$)$_2$-CH$_2$-CH$_2$-OH), 3.80–3.85 (m, 2H, CH$_3$-CH$_2$-CH$_2$-N(CH$_3$)$_2$-CH$_2$-CH$_2$-OH).

Synthesis of [N$_{1\ 1\ 2\ 2(OH)}$][C$_1$SO$_3$]. The procedure is similar to the one described above for the synthesis of the acetate-based ionic liquids, with the exception that the [N$_{1\ 1\ 2\ 2(OH)}$][OH] salt is used to titrate an equimolar aqueous solution of methylsulfonic acid. ^{1}H NMR was used to confirm the purity (99%) of the synthesized ionic liquids.

Table 1 List of ionic liquids used in the present study along with their stated purity and suppliers

Ionic liquid, origin, purity	Acronym	
1-Ethyl-3-methylimidazolium chloride, Iolitec, 98%	$[C_2mim]Cl$	
1-Butyl-3-methylimidazolium chloride, QUILL[13]	$[C_4mim]Cl$	
1-Hexyl-3-methylimidazolium chloride, QUILL[13]	$[C_6mim]Cl$	
1-Octyl-3-methylimidazolium chloride, QUILL[13]	$[C_8mim]Cl$	
1-Decyl-3-methylimidazolium chloride, QUILL[13]	$[C_{10}mim]Cl$	
1-Dodecyl-3-methylimidazolium chloride, QUILL[13]	$[C_{12}mim]Cl$	
1-Ethyl-3-methylimidazolium bromide, Fluka, 95%	$[C_2mim]Br$	
1-Ethyl-3-methylimidazolium acetate, Iolitec, 95%	$[C_2mim][CH_3COO] \equiv [C_2mim][Oac]$	
1-Ethyl-3-methylimidazolium ethylsulfonate, QUILL[14]	$[C_2mim][C_2H_5SO_3]$	
1-Ethyl-3-methylimidazolium triflate, Iolitec, 99%	$[C_2mim][CF_3SO_3] \equiv [C_2mim][Otf]$	
1-Ethyl-3-methylimidazolium hydrogensulfate, Iolitec, 99%	$[C_2mim][HSO_4]$	
1-Ethyl-3-methylimidazolium ethylsulfate, Iolitec, 99%	$[C_2mim][C_2H_5SO_4]$	
1-Ethyl-3-methylimidazolium octylsulfate, Merck,[15] 98%	$[C_2mim][C_8H_{17}SO_4]$	
1-Ethyl-3-methylimidazolium tetrafluoroborate, Solv.Innov., 98%	$[C_2mim][BF_4]$	
1-Ethyl-2,3-dimethylimidazolium tetrafluoroborate, Iolitec, 98%	$[C_2C_1mim][BF_4]^a$	
1-Ethyl-3-methylimidazolium thiocynate, Iolitec, 98%	$[C_2mim][SCN]$	
1-Ethyl-3-methylimidazolium dicynamide, Iolitec, 98%	$[C_2mim][N(CN)_2]$	
1-Butyl-3-methylimidazolium dicynamide, Iolitec, 98%	$[C_4mim][N(CN)_2]$	
1-Ethyl-3-methylimidazolium tetracyanoborate, Merck, 98%	$[C_2mim][B(CN)_4]$	
1-Butyl-3-methylimidazolium tricyanomethane, Merck, 98%	$[C_4mim][C(CN)_3]$	
Choline bis(trifluoromethane)sulfonamide, ITQB,[16] 99%	$[ch][N(CF_3SO_2)_2] \equiv [ch][Ntf_2]$	
Choline chloride, Sigma, 98%	$[ch]Cl$	
Choline dihydrogenphosphate, Iolitec, 98%	$[ch][H_2PO_4]$	
Ethylcholine acetate, ITQB	$[C_2ch][CH_3COO]^b$	
Propylcholine acetate, ITQB	$[C_3ch][CH_3COO]^b$	
Ethylcholine methylsulfonate, ITQB	$[C_2ch][CH_3SO_3]^b$	
Hydroxyethylcholine chloride, ITQB	$[ch(OH)_2]Cl^c$	
Hydroxyethylcholine bis(trifluoromethylsulfonyl)imide, ITQB	$[ch(OH)_2][N(CF_3SO_2)_2] \equiv [ch(OH)_2][Ntf_2]^c$	

QUILL = IL synthesized at Queen's University Ionic Liquid Laboratory, Belfast, UK. ITQB = IL synthesized at Instituto de Tecnologia Química e Biológica, Oeiras, Portugal (*cf.* materials). Choline = *N*-(2-hydroxyethyl)-*N,N,N*-trimethylammonium = $[N_{1\ 1\ 1\ 2(OH)}]^+$; Ethylcholine = *N,N*-dimethyl-*N*-ethyl-*N*-(2-hydroxyethyl)ammonium = $[N_{1\ 1\ 2\ 2(OH)}]^+$; Propylcholine = *N,N*-dimethyl-*N*-(2-hydroxyethyl)-*N*-propylammonium = $[N_{1\ 1\ 3\ 2(OH)}]^+$; Hydroxyethylcholine = *N,N*-di(2-hydroxyethyl)-*N,N*-dimethylammonium = $[N_{1\ 1\ 2(OH)\ 2(OH)}]^+$.

$[N_{1\ 1\ 2\ 2(OH)}][C_1SO_3]$. ^{1}H-NMR (DMSO-d$_6$, 400 MHz): δ/ppm = 1.24 (t, 3H, C$\underline{H}_3$-CH$_2$-N(CH$_3$)$_2$-CH$_2$-CH$_2$-OH), 2.31 (s, 3H, CH$_3$-(SO$_2$)-O), 3.03 (s, 6H, CH$_3$-CH$_2$-N(C$\underline{H}_3$)$_2$-CH$_2$-CH$_2$-OH), 3.35–3.42 (m, 4H, CH$_3$-C$\underline{H}_2$-N(CH$_3$)$_2$-CH$_2$-CH$_2$-OH), 3.79–3.83 (m, 2H, CH$_3$-CH$_2$-N(CH$_3$)$_2$-CH$_2$-C$\underline{H}_2$-OH), 5.27 (t, 1H, CH$_3$-CH$_2$-N(CH$_3$)$_2$-CH$_2$-CH$_2$-O$\underline{H}$).

Synthesis of $[N_{1\ 1\ 2(OH)\ 2(OH)}]Cl$. 2-Chloroethanol (1.1 mol equiv.) and 2-dimethyl-amino ethanol (1.0 mol equiv.) were mixed in a round-bottom flask, dissolved in *n*-hexane, under vigorous stirring, reflux and an N$_2$ atmosphere for several hours (monitored by ^{1}H NMR). The formation of the product can be observed by its precipitation from *n*-hexane. After completion of the reaction, the mixture was filtered and the reaction product was washed extensively with *n*-hexane in order to remove unreacted compounds and then dried under vacuum. The resulting $[N_{1\ 1\ 2(OH)\ 2(OH)}]Cl$ salt (yield 98%) was used without further purification. ^{1}H NMR was used to confirm the purity (99%) of the synthesized ionic liquid.

$[N_{1\ 1\ 2(OH)\ 2(OH)}]Cl$. ^{1}H-NMR (DMSO-d$_6$, 400 MHz): δ/ppm = 3.34 (s, 6H, (C$\underline{H}_3$)$_2$-N-(CH$_2$-CH$_2$-OH)$_2$), 3.54 (t, 4H, (CH$_3$)$_2$-N-(C$\underline{H}_2$-CH$_2$-OH)$_2$), 3.82–3.88 (m, 4H, (CH$_3$)$_2$-N-(CH$_2$-C$\underline{H}_2$-OH)$_2$), 5.35 (t, 2H, (CH$_3$)$_2$-N-(CH$_2$-CH$_2$-O$\underline{H}$)$_2$).

Table 1 also groups the different ionic liquids used in this work into different homologous series or interrelated sets that will be discussed below. Prior to their use all ILs were dried under vacuum and at moderate temperature for 48 h and their purity re-checked by ^{1}H NMR. Millipore water was used for preparation of the aqueous solutions. All the solutions were prepared using an Ohaus balance with ± 0.00001 g precision. The uncertainty in the reported molality values is ± 0.0001 molal.

Methods

The densities of the ionic liquid aqueous solutions and of pure water were measured using a DMA 5000 Anton Paar vibrating tube densimeter equipped with a temperature controller (Peltier device) with a precision of ± 0.001 °C and an overall density precision of ± 0.00001 g cm^{-3}. After careful injection of the sample into the densimeter (assuring that no bubble was left inside the vibrating tube), the temperature scan was set typically from 0 °C to 7 °C with a temperature step of 0.1 °C. At least 70 data points in this temperature range were registered for each sample. In the cases where the TMD was found to be lower than 0 °C, the freezing point depression for the corresponding solution was calculated and the lower value of the temperature range was set accordingly (in order to avoid freezing inside the vibrating tube). Typically each

temperature scan took around 4–5 h to complete, with the densimeter placed in a room thermostated at 15 °C.

Results

The density data are presented in Fig. 1. The figure is able to convey the large amount of data used to determine each TMD (each line comprises 70 or more independent data points whose density was recorded only after equilibration at each set temperature) and also the required precision of the measurement instrument—although all results are comprised between 0.9994 and 1.0102 g cm^{-3} it was necessary to expand and cut the y-scale into several segments in order to visualize the parabolic curvature of each run around the TMD of each solution.

The obtained density values were fitted to second order polynomials to obtain the corresponding temperatures at the maximum density of each run. The value obtained for the TMD of pure water is 3.98 °C, in excellent agreement with the values reported in the literature.[1] This confirms that the internal consistency and precision of the volumetric data are adequate for this type of determinations and that the calibration of the densimeter thermostat (with an estimated accuracy of only ±0.05 °C) will not impact adversely the $\Delta\theta$ results.

Two selected $\rho(T)$ plots from Fig. 1 are depicted in Fig. 2 (pure water and an ionic liquid aqueous solution where the TMD is below 0 °C) showing all individual data points, fitting curves and TMD values. It must be stressed that in some cases the $\rho(T)$ parabolic curve could only be measured mostly on one side of the density maximum due to the proximity of the
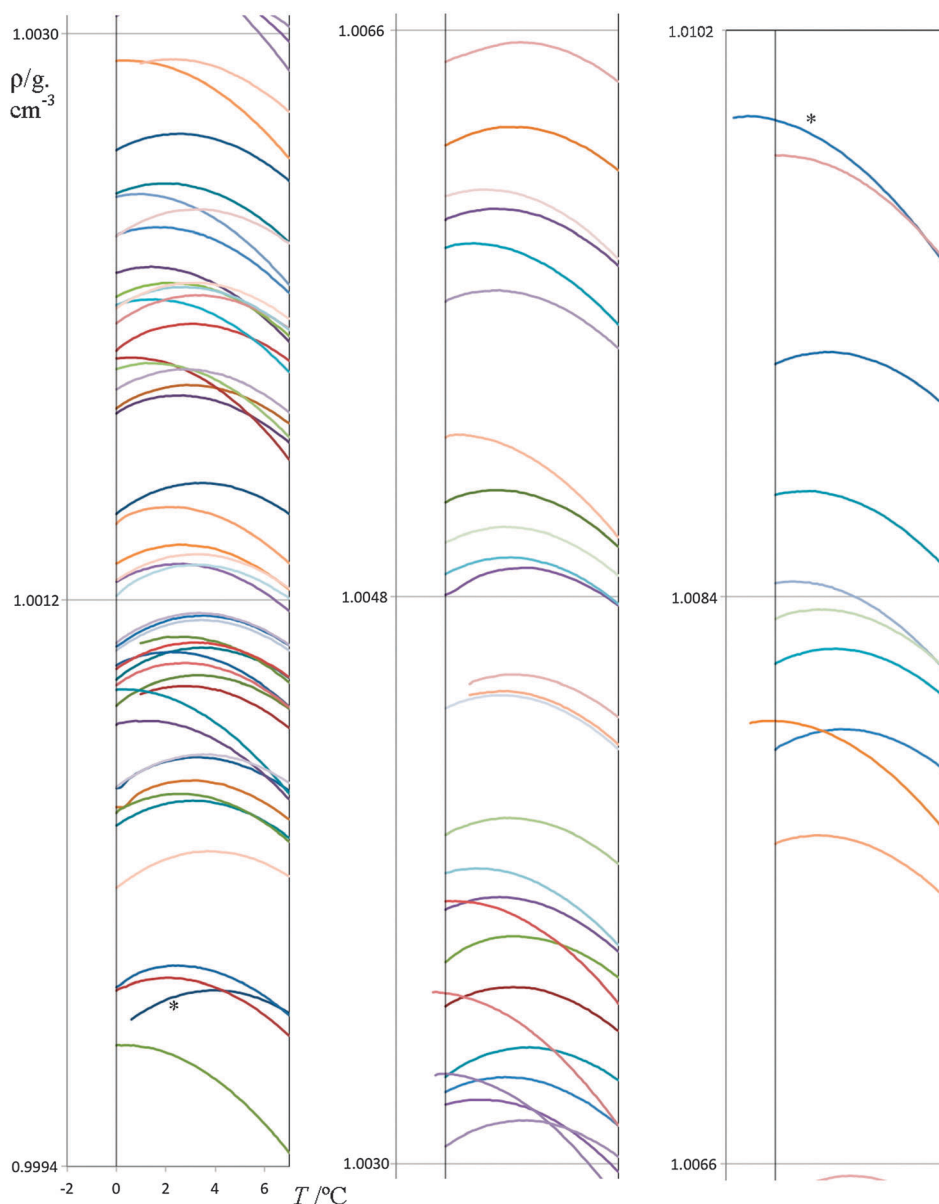

Fig. 1 Density as a function of temperature for each of the studied ionic liquid aqueous solutions. The two marked curves (*) are also shown in Fig. 2.
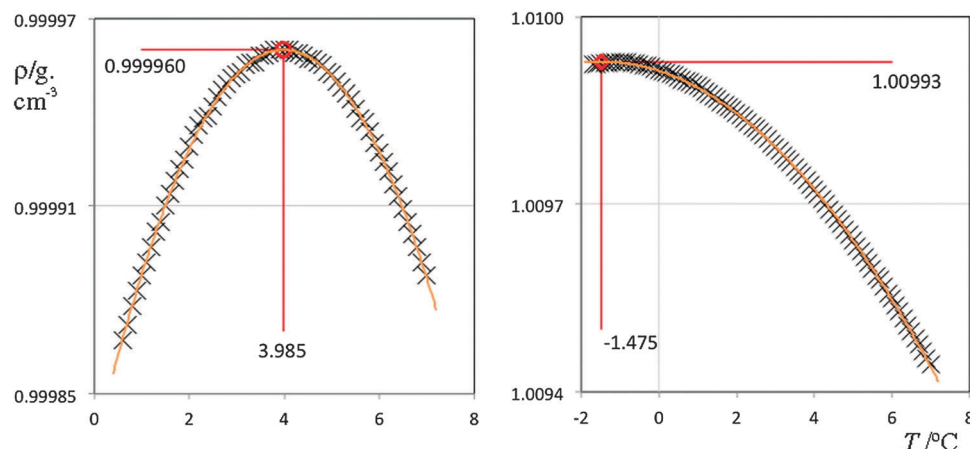
Fig. 2 Density as a function of temperature for pure water (left panel) and a 0.5 molal 1-ethyl-3-methylimidazolium acetate aqueous solution (right panel).

freezing point of the solution on the lower end of the selected temperature range. Nevertheless it was possible to measure TMD values below 0 °C due to the concurrent effect of the freezing point depression of the solutions (*cf.* Fig. 2, right side panel).

The obtained TMD data for all studied solutions are listed in Table 2. In order to address the impact of the ideal contribution to $\Delta\theta$ in each case (*cf.* Discussion section), the table also includes molar volume values of the pure ionic liquids, estimated at 298 K using the predictive method developed by Rebelo *et al.*[17]

Discussion

Alkyl side chain effects

The first group of ionic liquid aqueous solutions to be discussed comprises the 1-alkyl-3-methyl imidazolium chloride homologous series. Fig. 3 shows the TMD data along the series as a function of the concentration of the different solutions. The figure shows that the Despretz rule is observed for each member of the series and that the slope of the lines becomes more negative (larger $\Delta\theta$ effects) as the alkyl side chain in the

Table 2 TMD results for all studied ionic liquid aqueous solutions

Ionic liquid (V_m cm^3 mol^{-1})	TMD (solution molality)			
[C$_2$mim]Cl (125)	3.476 (0.056)	3.004 (0.105)	2.552 (0.152)	
[C$_4$mim]Cl (162)	3.320 (0.056)	2.579 (0.116)	1.994 (0.159)	
[C$_6$mim]Cl (197)	3.310 (0.043)	2.801 (0.072)	2.609 (0.084)	1.299 (0.161)
[C$_8$mim]Cl (229)	3.059 (0.043)	2.215 (0.085)	0.551 (0.161)	
[C$_{10}$mim]Cl (263)	2.566 (0.056)	1.137 (0.098)	0.075 (0.143)	
[C$_{12}$mim]Cl (297)	2.481 (0.075)	2.048 (0.096)	0.074 (0.212)	
[C$_2$mim]Br (159)	3.342 (0.060)	2.729 (0.114)	2.096 (0.167)	
[C$_2$mim][Oac] (155)	3.490 (0.056)	3.046 (0.104)	2.439 (0.166)	2.138 (0.193)
	0.926 (0.298)	−0.265 (0.402)	−1.475 (0.497)	
[C$_2$mim][C$_2$SO$_3$] (183)	3.311 (0.054)	2.608 (0.103)	2.034 (0.146)	
[C$_2$mim][Otf] (189)	3.132 (0.061)	2.371 (0.103)	1.459 (0.160)	
[C$_2$mim][HSO$_4$] (153)	2.261 (0.059)	0.664 (0.113)	0.080 (0.133)	
[C$_2$mim][C$_2$SO$_4$] (192)	3.169 (0.061)	2.590 (0.097)	1.740 (0.157)	
[C$_2$mim][C$_8$SO$_4$] (292)	2.813 (0.050)	1.275 (0.100)	0.315 (0.147)	
[C$_2$mim][BF$_4$] (154)	2.862 (0.065)	2.058 (0.105)	1.041 (0.151)	
[C$_2$C$_1$mim][BF$_4$] (166)	3.162 (0.047)	2.265 (0.098)	1.613 (0.135)	
[C$_2$mim][SCN] (152)	3.206 (0.071)	2.230 (0.134)	1.425 (0.190)	
[C$_2$mim][N(CN)$_2$] (167)	2.712 (0.058)	1.723 (0.102)	0.268 (0.163)	
[C$_4$mim][N(CN)$_2$] (189)	2.608 (0.058)	1.441 (0.105)	0.410 (0.143)	
[C$_2$mim][B(CN)$_4$] (218)	2.820 (0.032)	1.431 (0.067)	−0.413 (0.118)	
[C$_4$mim][C(CN)$_3$] (219)	2.255 (0.056)	0.809 (0.097)	−0.729 (0.144)	
[ch][Ntf$_2$] (252)	2.972 (0.045)			
[ch]Cl (119)	3.397 (0.058)	2.773 (0.114)	2.238 (0.162)	
[ch][H$_2$PO$_4$] (147)	2.785 (0.068)	1.809 (0.120)	0.507 (0.182)	
[C$_2$ch][Oac] (161)	3.812 (0.022)	3.475 (0.059)		
[C$_3$ch][Oac] (178)	3.590 (0.046)	3.331 (0.080)	3.241 (0.086)	
[C$_2$ch][C$_1$SO$_3$] (174)	3.268 (0.058)	2.500 (0.120)	0.475 (0.262)	
[ch(OH)$_2$][Ntf$_2$] (269)	2.786 (0.049)	0.711 (0.127)	−0.088 (0.168)	
[ch(OH)$_2$]Cl (136)	3.458 (0.045)	2.741 (0.106)	2.125 (0.155)	

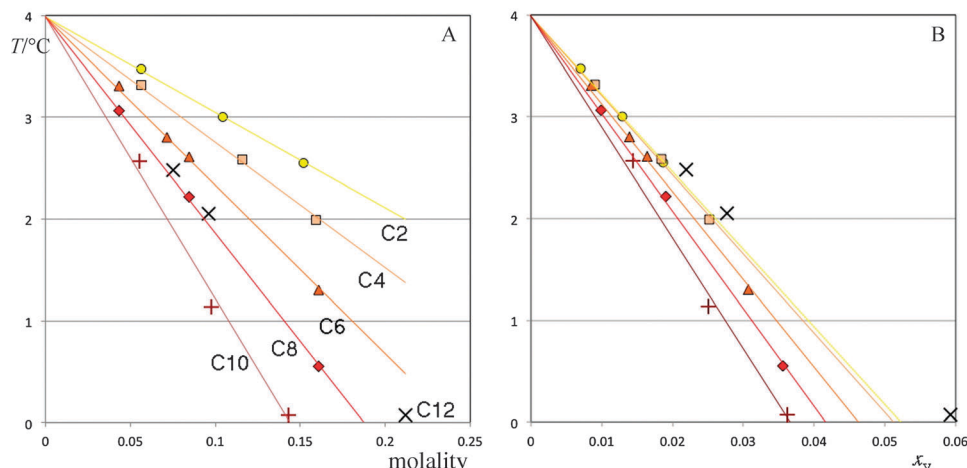**Fig. 3** TMD of [$C_n$mim]Cl aqueous solutions as a function of (A) molality and (B) solute volume fraction, x_V.

ionic liquid solute becomes longer. However this trend is interrupted in the case of the last member of the series, [C_{12}mim]Cl, that exhibits $\Delta\theta$ values lower than those of [C_{10}mim]Cl, and similar to those of [C_8mim]Cl.

Darnell and Greyson[4] have previously reported similar behavior for aqueous solutions of tetra-alkylammonium halide salts: in their case the TMD shifts for solutions of similar concentration follow the order $\Delta\theta([NH_4]Cl) < \Delta\theta([N(CH_4)_4]Cl) < \Delta\theta([N(C_2H_5)_4]Cl) < \Delta\theta([N(C_3H_7)_4]Cl) < \Delta\theta([N(C_4H_9)_4]Cl) < \Delta\theta([N(C_5H_{11})_4]Cl)$. The authors also discussed and resolved the apparent disagreement between the TMD data—that suggest that larger alkyl side chains break more efficiently the HB structure of water—and salting out-effect results show that at room temperature solutes with longer alkyl side chains are better structure promoters *via* the so-called hydrophobic effect; at room temperature the organization of water molecules around hydrophobic alkyl chains is an important effect because the fraction of loosely bound water molecules that can be locked into those structures is relatively high; at temperatures near the TMD of water most water molecules are still tightly hydrogen-bonded to other water molecules and the disruption of these structures and formation of the cage-like structures typical of the hydrophobic effect will not produce such a net positive structuring effect.[4]

This means that the alkyl side chain effects observed for [$C_n$mim]Cl ionic liquids near the TMD of water are caused by the influence of the size of the solute ions on the H-bonded structure of water rather than the usually structure-promoting or structure-disrupting effects observed at higher temperatures. This "elephant in a crystal shop" effect (larger elephants will produce larger disrupting effects) can be easily checked if Fig. 3A is re-plotted not as a function of molality but as a function of the volume fraction occupied by the solute molecules (x_V in Fig. 3B). In that case, if the comparisons are performed at similar solute volume fractions, the TMD shifts become much more similar to each other for solutes in the [C_2mim]Cl to [C_{10}mim]Cl range. The outlier character of [C_{12}mim]Cl is even more emphasized than in Fig. 3A.

Fig. 3B also shows that the shifts for [C_2mim]Cl and [C_4mim]Cl are almost identical and that only for [C_6mim]Cl to [C_{10}mim]Cl there is a regular increase in the slope of the TMD shifts with concentration. This seems to indicate that up to C4 the alkyl side chain is still strongly influenced by the charged part of the cation (the imidazolium ring) and that only from C6 onwards we have a more or less "independent" alkyl chain whose end is capable of disrupting *per se* the highly structured phase of liquid water near its TMD temperature. This inference agrees with simulation and X-ray data for different homologous series of pure ionic liquids,[12,18] which show that the segregation between a charged network and a continuous non-polar domain only starts to be effective for chains longer than five carbon atoms.

The outlier character of C12 can be rationalized if one takes into account not only Fig. 3B (for similar solute volume fractions the [C_{12}mim]Cl produce a TMD shift smaller than those of [C_2mim]Cl) but also the fact that for the studied solution concentrations the [C_{12}mim]Cl aqueous solution is probably above its critical micelle concentration (CMC)—at 298 K the CMC value is around 0.01 molal. In fact the effect of the C12 chains is smaller than their C2 counterparts simply because they are grouped inside micelles and hidden from the aqueous sub-phase.

Before continuing the discussion of the next group of ionic liquid solutes we would like to stress the fact that the amount of consistent thermal expansion coefficient data for pure ionic liquids is rather limited, especially if one considers whole homologous series like the just discussed [$C_n$mim]Cl solutes (the exceptions[19] are the [$C_n$mim][PF_6] and [$C_n$mim][Ntf_2] series that could not be considered in the present study due to their very low solubility values in water), and the temperatures at which one would need such data (around the TMD of water, where some of the neat studied ILs are solid). This lack of data prompted us to make the discussion not in terms of ideal *versus* structural shifts (the former quantity could not be calculated owing to the missing thermal expansion coefficient data) but to consider instead the shift dependence on the solute volume

fraction of the solutions. Such an approach also takes into account the shifts caused by the introduction of more or less bulky solute species that have to be accommodated in the highly structured frame of liquid water in the vicinity of its TMD temperature and needs only as input an estimate of the molar volume of the pure solute species (given in Table 2 for all studied IL solutes).

Anion effects

Fig. 4 shows the TMD shifts as a function of concentration for different aqueous solutions containing IL solutes composed of a common cation (1-ethyl-3-methylimidazolium ion) combined with different anions. Like in the previously discussed group of solutions, the Despretz rule is fairly observed throughout the set. The trends are always negative but represent quite differentiated types of behavior, ranging from weak TMD shifts to fairly strong ones; $\Delta\theta$ of just -1.4 °C for a 0.15 molal $[C_2mim][CH_3COO]$ solution versus $\Delta\theta$ of more than -4.4 °C for a $[C_2mim][HSO_4]$ solution with the same concentration. In fact the shifts cover the same temperature-molal composition area as those observed for the $[C_nmim]Cl$ solutions (alkyl side chain effects with $2 < C_n < 10$), cf. Fig. 4A. However, and unlike the previous effect where a homologous series was under discussion, it is not possible to establish an obvious relation between the different trends and the nature of the anions.

Nevertheless, the first step towards the rationalization of the anion effect lies again in the representation of the TMD shifts as a function of the volume fraction of the solution occupied by the solute ions. Such representation is shown in Fig. 4B. One of the most interesting facts that emerges from the figure is that the effect from four of the anions—Cl^-, Br^-, $[C_2H_5SO_4]^-$ and $[C_2H_5SO_3]^-$—collapse into a single trend if their different sizes are taken into account. Further two ions, $[C_8H_{17}SO_4]^-$ and $[CF_3SO_3]^-$, show slightly more intense shifts but still inside the range predicted by the hydrophobic effects associated with

longer alkyl side chains or (in the case of $[CF_3SO_3]^-$) the presence of a fluorinated alkyl moiety.

Two of the remaining six anions, $[CH_3COO]^-$ and $[HSO_4]^-$, show the lowest and highest TMD shifts, respectively, represented by the two trend-lines of Fig. 4B. This situation is probably related to the fact that these two anions are the conjugated bases of two very different acids (acetic acid, a weak organic acid and sulfuric acid, a strong diprotic inorganic acid) with very different proton donor/acceptor characteristics. These will be discussed in the next topic, concerning the direct influence of proton acceptors/donors on the TMD shifts of water.

The last four anions—$[SCN]^-$, $[N(CN)_2]^-$, $[B(CN)_4]^-$ and $[BF_4]^-$—exhibit relatively strong shifts taking into account their relative sizes. The nitrile-based homologous series shows monotonous behavior, showing progressively larger shifts as the number of nitrile groups in the ion increases: $\Delta\theta([C_2mim][SCN]) < \Delta\theta([C_2mim][N(CN)_2]) < \Delta\theta([C_2mim][B(CN)_4])$. Unfortunately the $[C_2mim][C(CN)_3]$ ionic liquid is not available in order to complete the series, but since it was shown that the influence of C2 or C4 chains is almost the same, we have decided to compare the data on those ions with the results obtained for $[C_4mim][N(CN)_2]$ and $[C_4mim][C(CN)_3]$.

Fig. 5 shows that if the different sizes of the ions are taken into account there is indeed a strong correlation between the number of nitrile groups and the power of the corresponding ionic liquid to break more effectively the structure of water near its TMD. Still in this context, the last ionic liquid under discussion, $[C_2mim][BF_4]$, (structurally similar to $[C_2mim][B(CN)_4]$) shows $\Delta\theta$ values in the range shown in Fig. 5 (similar to those of $[C_2mim][N(CN)_2]$).

The relatively strong disrupting behavior of these ions is in agreement with different correlations that try to establish different hydrophobicity scales for ionic liquids.[20,21] For instance Ranke and co-workers[20] established that ionic liquids based on $[SCN]^-$, $[BF_4]^-$, $[C(CN)_3]^-$ and $[B(CN)_4]^-$ show a progressively
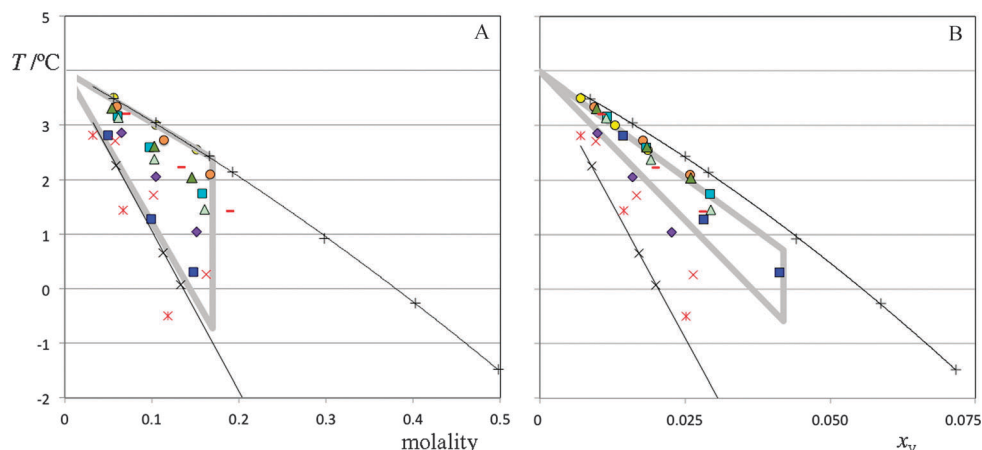

Fig. 4 TMD of $[C_2mim]\times$ aqueous solutions as a function of (A) molality and (B) solute volume fraction, x_V. The different anions (X^-) are labeled according to the following colors and symbols: Cl^- = yellow circles; Br^- = orange circles; $[CH_3COO]^-$ = black crosses; $[HSO_4]^-$ = black ×s; $[C_2H_5SO_4]^-$ = cyan squares; $[C_8H_{17}SO_4]^-$ = blue squares; $[C_2H_5SO_3]^-$ = green triangles; $[CF_3SO_3]^-$ = light green triangles; $[SCN]^-$ = red bars; $[N(CN)_2]^-$ = red ×s; $[B(CN)_4]^-$ = red stars; $[BF_4]^-$ = purple rhomb. The two black trend lines show the limiting behavior of the $[C_2mim][CH_3COO]$ and $[C_2mim][HSO_4]$ aqueous solutions. The grey triangles mark the range of the alkyl side chains TMD effects discussed in the previous paragraph (cf. also Fig. 3).
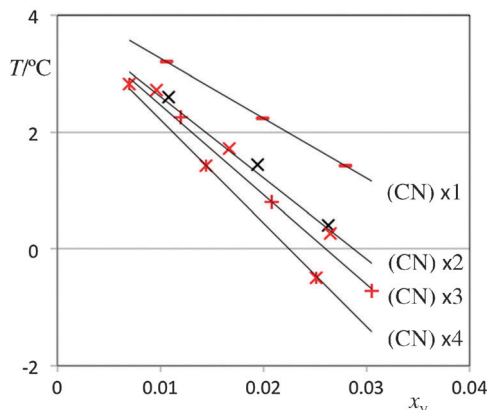
Fig. 5 TMD of selected [C₂mim]× and [C₄mim]× aqueous solutions as a function of solute volume fraction, x_V. All anions (X⁻) show different degrees of nitrile substitution: [C₂mim][SCN] = red bars; [C₂mim][N(CN)₂] = red ×s; [C₄mim][N(CN)₂] = black ×s; [C₄mim][C(CN)₃] = red crosses; [C₂mim][B(CN)₄] = red stars.

larger hydrophobic character, in agreement with the present $\Delta\theta$ results. It must be stressed that there are anions with even more pronounced hydrophobic character like $[PF_6]^-$ or $[Ntf_2]^-$. However, the 1-alkyl-3-methylimidazolium-based ionic liquids of those anions show very small solubilities in water, which curtails the measurement of the corresponding TMD shifts. Conversely, anions that exhibit lower $\Delta\theta$ results such as the halides, alkylsulfates or alkylsulfonates (Fig. 4B) are those at the "hydrophilic" end of such scales.[21]

Hydrogen bond effects

All TMD shifts discussed so far represent negative deviations from the TMD of pure water. In fact, TMD shifts involving aqueous solutions of ionic solutes are in general always negative. Even in the case of molecular solutes only a few systems exhibit positive shifts in the most diluted regimes—as stated in the Introduction, ethanol and propanol solutions are two of the most well-known examples. Such a state of affairs reflects the

usually more important contributions to the TMD shifts of the negative $\Delta\theta_{id}$ ideal terms.

One of the most effective ways to study TMD effects in aqueous solutions of molecular solutes has been to separate the $\Delta\theta$ values in their corresponding ideal and structural terms ($\Delta\theta = \Delta\theta_{id} + \Delta\theta_{st}$) and use volumetric data for the pure solutes to evaluate the different structural contributions:

$$\Delta\theta_{st} = \Delta\theta - \Delta\theta_{id} = \Delta\theta - (x_2\,\alpha_{p,2}\,V_2)/(2x_1\,\alpha_{p,1}\,V_1), \quad (1)$$

where the 1 and 2 subscripts refer to the solute and water, respectively, and x, α_p and V are the mole fraction, thermal expansion coefficient and molar volume, respectively. Such an approach tends to emphasize the different nature of the structural shifts (even when the overall shift is negative the structural shift can be either positive or negative) and has allowed many different rationalizations of the observed effects in terms of the underlying solute–water interactions, namely hydrogen-bonding between solute and water molecules.[4,5,9] In the case of alcohol and amine molecules it was found that molecules with compact alkyl residues and groups that can act simultaneously as proton donors and acceptors (the hydroxyl group of alcohols, the NH group of secondary and primary amines) can participate in the formation of water clathrate structures, thus yielding a positive $\Delta\theta_{st}$ contribution.[5] In the case of ethanol, propanol or di-sec-butylamine such contributions are larger than the ideal term and originates the above-mentioned positive TMD shifts.

The last group of IL solutes to be discussed includes cations based on the cholinium ion (a tetra-alkyl ammonium ion where one of the alkyl chains is substituted with a hydroxyl group at the C2 position). Such a type of ions highlights the possibility of simultaneous hydrogen-bonding and electrostatic interactions between water and the solute species. Fig. 6A shows the temperature–concentration diagram (plotted as a function of solute volume fraction) of seven choline-based IL aqueous solutions. Fig. 6B compares three of those IL solutions with the most differentiated TMD shifts ([Ch][H₂PO₄], [C₂Ch][CH₃COO] and
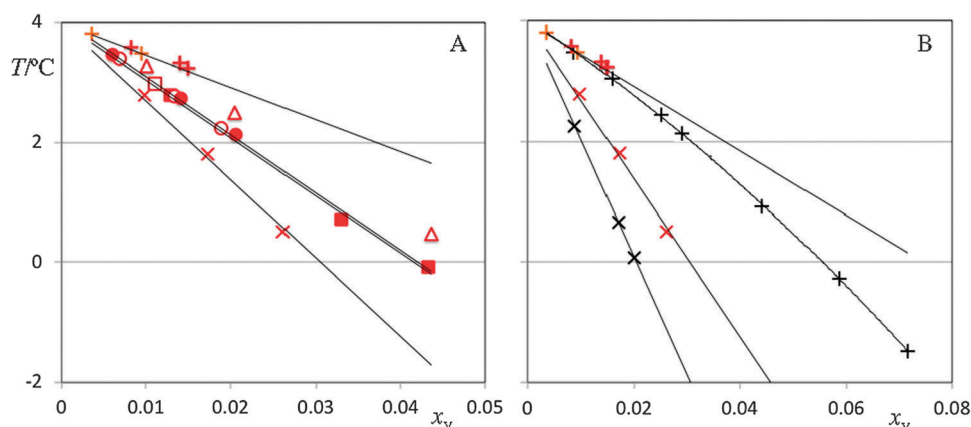

Fig. 6 TMD of selected choline-based IL aqueous solutions as a function of solute volume fraction, x_V. The different ions are labeled according to the following colors and symbols (A): [Ch][Ntf₂] = empty squares; [Ch(OH)₂][Ntf₂] = filled squares; [Ch]Cl = empty circles; [Ch(OH)₂]Cl = filled circles; [C₂Ch][CH₃SO₃] = empty triangles; (A and B) [Ch][H₂PO₄] = red ×s; [C₂Ch][CH₃COO] = red crosses; [C₃Ch][CH₃COO] = orange crosses; (B) [C₂mim][CH₃COO] = black crosses; [C₂mim][HSO₄] = black ×s.

[C$_3$Ch][CH$_3$COO]) with their counterparts based on the imidazolium cations ([C$_2$mim][CH$_3$COO] and [C$_2$mim][HSO$_4$]).

One of the most interesting characteristics of cholinium-based ILs is the possibility of preparing moderately water-soluble ILs based on hydrophobic anions such as [Ntf$_2$]$^-$. Accordingly we were able to measure the TMD shifts in [Ch][Ntf$_2$] and [Ch(OH)$_2$][Ntf$_2$]. Although the overall $\Delta\theta$ values for those two ILs are as intense as those of [C$_2$mim][C$_8$H$_{17}$SO$_4$], the shifts become similar to those of the hydrophilic [Ch(OH)$_2$]Cl IL (Fig. 6A) when the bulky size of the [Ntf$_2$]$^-$ anion is duly taken into account. The slopes are in fact not very different from those already encountered in Fig. 3B and 4B. This means that the disruption of the water structure caused by the hydrophobic nature of the [Ntf$_2$]$^-$ anion has to do more to its size and the existence of the terminal trifluoromethyl groups than to any type of detrimental specific interactions with its charged moieties. In fact, Koga and co-workers[21] have shown that this particular anion can act as an amphiphile towards water, with relatively important and simultaneous hydrophilic and hydrophobic contributions (generally won by the latter). Probably the presence of the cholinium cation (either mono- or di-hydroxy substituted) helps to shift such balance towards a more effective interaction with water.

The second point to be discussed is the fact that in the case of chloride- and sulfonate-based ILs there is not much difference in terms of the corresponding TMD shifts between the cholinium and the 1-ethyl-3-methylimidazolium ILs (triangles and circles in figures in Fig. 4B and 6A). Apparently for these hydrophilic anions the presence of hydroxyl ions in the cation does not change the dominating effect produced by the modification of the water structure *via* electrostatic interactions with the anions. This also seems to be the case for [C$_2$Ch][CH$_3$COO] and [C$_3$Ch][CH$_3$COO] *versus* [C$_2$mim][CH$_3$COO]—the ILs with the lowest observed TMD shifts. However, (i) the curvature of the TMD plots for the extended measurement range in the case of the [C$_2$mim][CH$_3$COO] systems (a detectable deviation from the Despretz rule) suggests that the contributions from the $\Delta\theta_{st}$ term are less negative for the solutions with lower concentrations (implying a more stabilized water structure); and (ii) such stabilization is slightly more important in the systems containing the choline cation (an extra hydroxyl group). In fact the acetate ion is, among all studied anions, the one whose negative centers (delocalized between the two oxygen atoms) can act more efficiently as proton acceptors (the acetate anion is in fact a relatively strong base) and promote effective hydrogen bonds with water. The presence of hydroxyl groups in the cation—that can also act as proton donors—can help such stabilization, as in the case of molecular solutes such as alcohols or primary and secondary amines.

Finally, the largest difference in TMD shifts between imidazolium- and choline-based ILs was found between aqueous solutions containing [C$_2$mim][HSO$_4$] and [ch][H$_2$PO$_4$] solutes. These are also the systems where the volume-corrected TMD shifts are larger, indicating the largest destabilization effects in the structure of water. Both anions are the conjugated bases of polyprotic strong acids, *i.e.*, the proton acceptor capability of the anions is very low. Moreover, in aqueous solution both ions can participate in equilibria with further dissociated species ([SO$_4$]$^{2-}$, [HPO$_4$]$^{2-}$). The possible formation of divalent anions will impact the structure of water not only because of enhanced electrostatic interactions (that as we have seen for most ions tend to destabilize the structure of water) but also through the modification of the overall pH of the solution. The presence of OH groups in the cation offsets these effects and leads to a more subdued TMD shift ($\times$s in Fig. 6B).

Other effects

Two additional pairs of IL solutes can provide further insights concerning two other types of (minor) TMD shift effects; the [C$_2$mim][BF$_4$]–[C$_2$C$_1$mim][BF$_4$] pair illustrates the modification of the proton donor capability of the imidazolium cation through the substitution of its most acidic hydrogen atom by a methyl group; the [C$_2$mim][CH$_3$SO$_3$]–[C$_2$mim][CF$_3$SO$_3$] pair deals with the stabilization of the anion as a weaker base *via* the substitution of a methyl group by a more electron-withdrawing group (–CF$_3$).

In the latter case the shifts are already depicted in Fig. 4 and show that even if the different size of the two anions is taken into account (Fig. 4B), the [C$_2$mim][CF$_3$SO$_3$] solute produces slightly larger shifts than its non-fluorinated counterpart. This is in good agreement with the arguments advanced in the previous section: (i) a weaker base is less eager to accept protons and became a part of the hydrogen-bonded network; (ii) electrostatics without a concomitant proton acceptor/donor capability result in a reorganization of the water molecules around the ions, the loss of its ice-like open structure and more negative $\Delta\theta$ values; and (iii) triflate-based ionic liquids are less water-soluble ("more hydrophobic") than the analogous methyl sulfonate salts.

In the case of the [C$_2$mim][BF$_4$]–[C$_2$C$_1$mim][BF$_4$] pair almost no effect in the $\Delta\theta$ trends is observed when the substitution takes place (the shifts are both quite intense given the hydrophobic nature of the common [BF$_4$]$^-$ anion, *cf.* Table 2). This suggests that in the case of imidazolium-based ILs, the water–cation interactions are less important than the corresponding water–anion interactions.

Conclusions

The present work measured and discussed for the first time shifts in the TMD of water caused by ionic liquid solutes. A vast amount of high-precision volumetric data allowed us to analyze the TMD shifts for different homologous series or similar sets of ionic solutes and explain the overall effects in terms of hydrophobic, electrostatic and hydrogen-bonding contributions.

One of the main advantages of using ILs as probes to investigate the TMD shifts in aqueous solutions is the fact that this class of compounds can be tailored in order to modulate the three types of contribution mentioned in the previous paragraph: longer alkyl chains in the cations or anions can yield larger hydrophobic effects; anions can exhibit different degrees of charge dispersion/hydrophilicity; OH groups can be

added to the cations in order to promote further hydrogen-bonding interaction centers. Moreover, unlike many molecular solutes, many ILs with extended alkyl chains show extended miscibility windows in water ([C$_8$mim]Cl is completely miscible in water whereas octanol is barely soluble) and, unlike traditional inorganic salts, their solubility in water will not be controlled by the stability of the corresponding crystalline solids (upon reaching their solubility limit ILs do not precipitate but form a second IL-rich liquid phase).

The analysis of the TMD shift data in the [C$_n$mim]Cl homologous series and the plotting of the temperature–concentration diagrams as a function of solute mole fraction have shown that the structuring of water around alkyl chains (hydrophobic effect) destabilizes the underlying structure of pure water (still partially ice-like) in the vicinity of its TMD and that the destabilization is dominated by size effects. When the IL solutes start to form micelles (in the case of [C$_{12}$mim]Cl) such trends are reversed due to the segregation of the alkyl chains from the aqueous media. It must be stressed that such hydrophobic effects in many cases lead to the structuration of water molecules around hydrophobic molecules and can contribute to salting-out effects in aqueous solutions at higher temperatures produce a very different outcome when considering liquid water in the vicinity of its TMD temperature; in the case of aqueous solutions around room-temperature the free water molecules that are stabilized around the organic solutes promote an overall structuration of the aqueous solution and can lead to salting-out effects; in the case of the highly structured water near its TMD the formation of structures around organic molecules is detrimental to the overall structure of water—the two types of structures are ill-matched.

The same type of argument applies to the organization of water molecules around ionic solutes; if the ions cannot participate in a "compatible" way with the pre-existing (still partially ice-like) hydrogen bond network of liquid water near its freezing point, then the formation of the 16 solvation shells around the ions will have an overall negative effect concerning the stability of structured media. The study of anion effects on the TMD of IL aqueous solutions has shown that the hydrophilicity/hydrophobicity scales usually used to describe the anions of ionic liquids reflect the intensity of the TMD shifts of the corresponding IL solutes. Anions with very strong and/or isotropic electrostatic interaction centers tend to rearrange water molecules around them in a way that disrupts the open hydrogen-bond network of pure water at temperatures around the TMD, whereas those with more dispersed and tetrahedral-oriented interaction centers tend to preserve such a network.

Finally the introduction of additional OH groups seems to have little effect in terms of the TMD shifts of the aqueous solutions containing the most hydrophilic IL, whereas the reverse is true for their hydrophobic counterparts. In the cases where the influence of added hydroxyl groups is noticeable the changes are always in the direction of more subdued TMD shifts; the added OH groups (not centered in the electrostatic interaction centers) will help in the stabilization of the open hydrogen-bonded network of water in the TMD vicinity.

Interestingly, the TMD shifts caused by adding bulky ions to water are commensurate with those of applying positive pressure to neat water, where one finds a 2 K negative shift in the TMD per 10 MPa of applied pressure.[22] On the other hand, further studies,[23] namely in IL solutions of deuterated water, are being currently explored in order to further elucidate the relation between the strength of the hydrogen-bonded network of water and its destabilization by the different types of anion discussed in this work—more hydrophobic ([Ntf$_2$]$^-$, [BF$_4$]$^-$ or [B(CN)$_4$]$^-$), more hydrophilic ([CH$_3$SO$_4$]$^-$ or Cl$^-$), or even hydrophilic with the possibility of proton transfer ([CH$_3$COO]$^-$).

Acknowledgements

References

1 M. F. Cawley, D. McGlynn and P. A. Mooney, *Int. J. Heat Mass Transfer*, 2006, **49**, 1763–1772.

2 M. Despretz, *Ann. Chim. Phys.*, 1839, **70**, 49–81.

3 M. Despretz, *Ann. Chim. Phys.*, 1840, **73**, 296–310.

4 A. J. Darnell and J. Greyson, *J. Phys. Chem.*, 1968, **72**, 3021–3025.

5 F. Franks and B. Watson, *Trans. Faraday Soc.*, 1967, **63**, 329–334.

6 D. D. Macdonald, M. E. Estep, M. D. Smith and J. B. Hyne, *J. Solution Chem.*, 1974, **3**, 713–725.

7 D. D. Macdonald, B. Dolan and J. B. Hyne, *J. Solution Chem.*, 1976, **5**, 405–416.

8 D. D. Macdonald, A. McLean and J. B. Hyne, *J. Solution Chem.*, 1978, **7**, 63–71.

9 D. D. Macdonald, A. Maclean and J. B. Hyne, *J. Solution Chem.*, 1979, **8**, 97–103.

10 T. S. Sarma and J. C. Ahluwalia, *J. Phys. Chem.*, 1970, **74**, 3547–3551.

11 A. A. H. Pádua, M. F. Costa Gomes and J. N. A. C. Lopes, *Acc. Chem. Res.*, 2007, **40**, 1087–1096.

12 J. N. A. C. Lopes and A. A. H. Pádua, *J. Phys. Chem. B*, 2006, **110**, 3330.

13 M. Blesic, M. H. Marques, N. V. Plechkova, K. R. Seddon, L. P. N. Rebelo and A. Lopes, *Green Chem.*, 2007, **9**, 481–490.

14 M. Blesic, M. Swadźba-Kwaśny, J. D. Holbrey, J. N. C. Lopes, K. R. Seddon and L. P. N. Rebelo, *Phys. Chem. Chem. Phys.*, 2009, **11**, 4260–4268.

15 A. J. L. Costa, J. M. S. S. Esperança, I. M. Marrucho and L. P. N. Rebelo, *J. Chem. Eng. Data*, 2011, **56**, 3433–3441.

16 A. J. L. Costa, M. R. C. Soromenho, K. Shimizu, I. M. Marrucho, J. M. S. S. Esperança, J. N. C. Lopes and L. P. N. Rebelo, *J. Phys. Chem. B*, 2012, **116**, 9186–9195.

17 L. P. N. Rebelo, J. N. C. Lopes, J. M. S. S. Esperança, H. J. R. Guedes, J. Łachwa, V. Najdanovic-Visak and Z. P. Visak, *Acc. Chem. Res.*, 2007, **40**, 1114–1121.

18 A. Triolo, O. Russina, H.-J. Bleif and E. Di Cola, *J. Phys. Chem. B*, 2007, **111**, 4641–4644.

19 M. Tariq, P. A. S. Forte, M. F. C. Gomes, J. N. C. Lopes and L. P. N. Rebelo, *J. Chem. Thermodyn.*, 2009, **41**, 790–798.

20 J. Ranke, A. Othman, P. Fan and A. Müller, *Int. J. Mol. Sci.*, 2009, **10**, 1271–1289.

21 H. Kato, K. Nishikawa and Y. Koga, *J. Phys. Chem. B*, 2008, **112**, 2655–2660.

22 H. I. M. Veiga, L. P. N. Rebelo, M. Nunes da Ponte and J. Szydlowski, *Int. J. Thermophys.*, 2001, **22**, 1159.

23 M. Tariq, J. M. S. S. Esperanca, L. P. N. Rebelo and J. N. C. Lopes, *Molecules*, 2013, **18**, 3703–3711.